

Cell SoC Balancing Using a Cascaded Full Bridge Multilevel Converter in Battery Energy Storage Systems

Efstathios Chatzinikolaou, *Student Member, IEEE* and Daniel. J. Rogers, *Member, IEEE*

Abstract— This paper presents a method for achieving individual electrochemical cell balancing by using a cascaded full bridge multilevel converter where a single electrochemical cell is connected to each converter module. As a result, balancing at cell level is possible without additional circuitry, making this topology ideal for long service life grid storage and applications using second-life cells where the cells are inherently poorly matched. In order to estimate the relative state of charge between cells, the control flexibility of the multilevel converter is used to remove each cell from the current path without interrupting the operation of the system. This process eliminates the effect of the internal cell resistance and fast transient electrochemical phenomena and therefore the measured voltage serves as a high quality ‘pseudo open circuit’ voltage measurement. The proposed balancing strategy is validated using a 25 level cascaded full bridge multilevel converter prototype for the individual balancing of twelve lithium polymer cells, during consecutive charging and discharging cycles. Successful balancing to within 5 mV of open circuit voltage is observed between cells with 45% difference in nominal capacity and 55% initial state of charge variation.

Index Terms— Cell balancing, lithium-ion battery, multilevel converter, open-circuit voltage

I. INTRODUCTION

LARGE scale battery Energy Storage Systems (BESS) facilitate the integration of renewables by providing arbitrage and a number of ancillary services such as voltage and frequency regulation [1]. Conventionally, the BESS is integrated to the AC grid via single-stage or two-stage DC-AC converter topologies [2]. In order to achieve the required battery voltage and current ratings, cells are connected in series and in parallel [3]. Differences between cell parameters

within a pack must be expected, even between seemingly identical cells, due to variations in the manufacturing process or during operation (pack temperature variations, aging effects) [4]. When charging a pack of cells connected in series, the cell with the lowest capacity will be the first to reach the maximum voltage limit and terminate the charging process while the rest of the cells are not fully charged. Conversely when discharging, the cell with the lowest capacity will reach first the cut-off voltage and terminate the discharge while there is still charge available in the pack. In order to fully utilise the available capacity of the battery pack a balancing circuit is required [5]. Cell balancing is either passive, where balancing is achieved by dissipating excess energy through resistors or active, where additional storage devices such as capacitors or inductors are used to achieve balancing by transferring energy between the cells of the pack [6]. Cell balancing is performed either by using cell terminal voltages or cell state of charge (SoC). In this paper the term balancing refers to SoC balancing unless otherwise specified.

The success of a balancing strategy depends on accurate SoC estimation. SoC is the available capacity of a cell as a percentage of the total capacity of the cell. Ampere Hour Balancing (AHB) is a straightforward method of calculating SoC by integrating the cell current. However, this method requires previous knowledge of the cell capacity and the initial SoC and can suffer from cumulative measurement error during current integration [7]. Another approach is SoC calculation based on the open circuit voltage (OCV) of the cell [8, 9]. In order to acquire accurate OCV measurements the cell should be rested for a long period of time (as long as 24 hours) which is not possible while the system is operating. For more accurate SoC estimation, electrochemical models of the cell or equivalent circuit models can be used in combination with adaptive filters and observers (Kalman, sliding mode observer) [10-12] but due to high complexity it is difficult to implement for many thousands of individual cells in large scale systems.

Modular Cascaded Full Bridge also known as Cascaded H-Bridge (CHB) multilevel converter topologies (Fig. 1a) are emerging in BESS applications because of their advantages of using low voltage semiconductor switches, producing low

Manuscript received January 29, 2016; revised March 11, 2016; accepted April 08, 2016. This work was supported in part by the UK Engineering and Physical Sciences Research Council under grant EP/K002252/1.

E. Chatzinikolaou and D. J. Rogers are with the Energy and Power Group, Department of Engineering Science, University of Oxford, Oxford, U.K. (e-mail: efstratios.chatzinikolaou@worc.ox.ac.uk).

output voltage harmonic distortion and inherent modularity leading to simple voltage scaling properties. CHB converters provide an ability to achieve SoC balancing between the phases and between the sub modules of a phase without using additional balancing circuits [13-19]. In [17] a single phase CHB multilevel converter with battery balancing is presented. A battery pack is connected to each one of the full bridge converters of the cascaded topology and balancing is achieved by controlling the duty cycle of each module. The balancing is based on pack terminal voltage measurements. The drawback of this method is that voltage measurements cannot provide an accurate estimation of SoC due to the voltage error introduced by the internal resistance and the transient electrochemical phenomena. Moreover, balancing within the battery pack of each module is not addressed. In [18] an active power control of individual converter cells for a BESS based on a CHB converter is presented. Each converter cell is connected to a battery pack and balancing is achieved between the three phases by controlling the zero voltage component of the output voltage while the power output of each module is decided based on their respective SoC. The process of SoC estimation as well as balancing within the battery pack requires an additional battery management system (BMS). In [19] a multi-level BMS is developed for a CHB BESS. Phase balancing and module balancing is achieved by using the multilevel converter topology as in the previous cases. Balancing at pack level is realised by using additional DC-AC inverters and at cell level by using a multi-winding transformer. SoC is estimated using a combination of an equivalent circuit model combined with an Extended Kalman filter but due to the complexity of the applied method, SoC is estimated for each pack rather than each individual cell.

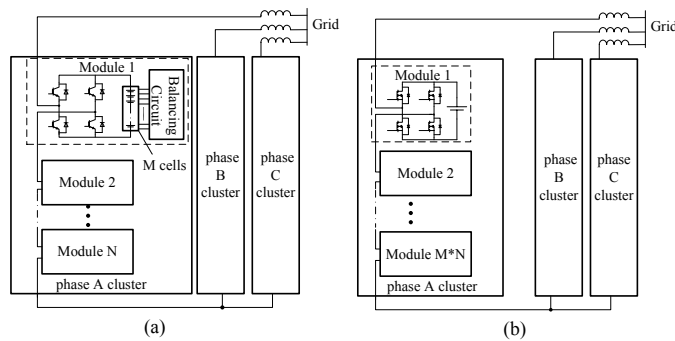


Fig. 1. (a) Conventional cascaded full bridge multilevel converter BESS (b) Cascaded full bridge multilevel converter BESS with single cell per sub module.

This paper presents a new approach to a BESS using a CHB multilevel converter where each converter module is connected to a single cell rather than a pack of cells (Fig. 1b). This configuration enables individual monitoring and control of each electrochemical cell and thus SOC balancing can be achieved at the lowest level of the BESS without any additional balancing circuits. The reliability of the system becomes much less dependent on the reliability of the cells since cell failure can be managed on-line by isolating a single cell rather than the whole pack. Finally, the modularity of the

multilevel topology is utilised in order to perform cell balancing using pseudo-open circuit voltage measurements (POCV).

Despite the advantages mentioned above, the implementation of the single cell per H-bridge topology may be challenging for a BESS with large numbers of cells. The key challenges are circuit complexity and management of power losses in the converter. The control complexity of such a system is addressed in [20] where the balancing of 2835 cells is achieved by using a hierarchical control strategy. In the CHB multilevel circuit switching losses are essentially zero because the MOSFETs are switched at only twice the fundamental frequency. Conduction losses in a single H-bridge can be reduced by using MOSFETs with low on-state resistance. However, when using only a single cell in each H-bridge, the blocking voltage of even the lowest voltage-rated commercial MOSFETs is significantly underutilised (i.e. cell voltage of 3-4.2 volts compared to 20V automotive-class MOSFETs). As a result, the proposed topology is mainly attractive for applications where individual monitoring and control of each cell is a high priority such as long service life grid storage where cells may be used for decades, or applications using second-life cells which are inherently poorly matched.

Second-life batteries can be used in grid storage applications, creating a revenue opportunity that can improve the return of investment. Automotive manufacturers recommend battery replacement when the capacity drops between 70-80% [21] leaving plenty of scope for use in other less demanding applications. Due to the wider spread in the characteristics of second life cells, a modular converter design using a DC/DC converter for each cell is proposed in [22], in order to enable connection of large number of cells, maximize the use of available capacity and minimize the degradation of the re-used cells.

Another way to gain individual control over cells is to build an “electronics-enabled” battery pack such as the one presented in [23]. This pack configuration uses additional MOSFETs in series with each cell and in parallel with each module, controlled by a BMS in order to enable self-healing from single cell failures as well as individual cell balancing. This system also includes an additional two-stage converter topology for DC to AC conversion.

In summary, extra circuitry is *always* required to provide monitoring and balancing at an individual cell level. The additional capacity utilisation and improvements in reliability gained as a result must be traded against the cost of this additional circuitry on an application by application basis. The advantage of the CHB multilevel converter is that it provides similar controllability to the above [22, 23] and also an in-built DC-AC conversion capability. All such methods generally become more attractive when using larger, high-value cells (>20Ah) because the sensing and control circuits become a smaller fraction of the total cost of the system.

This paper is organised as follows; the balancing strategy using the multilevel topology is presented in Section II. The concept of using POCV measurements for cell balancing and

the attendant calculation of the idle state duration are described in Section III. The MATLAB simulation results for the POCV balancing of twelve cells are presented in Section IV. The description of the converter control and the implemented balancing algorithm are presented in Section V. The experimental process followed is described in Section VI and the results of individual balancing of twelve lithium polymer cells during consecutive charge and discharge cycles, using a 25-level single-phase CHB multilevel converter are discussed in Section VII. Finally, conclusions are drawn in Section VIII.

II. BALANCING USING A CASCADED FULL BRIDGE MULTILEVEL CONVERTER

In the cascaded multilevel converter, an output voltage close to a sinusoidal reference is produced by switching on and off the converter modules to create a stepped output voltage. In Fig. 2 the output voltage of a 13 level multilevel converter (green line) is constructed based on a sinusoidal voltage reference (blue line). This operation results in each cell experiencing different duty cycles (i.e. the fraction of time each cell is placed in the load current path) and therefore varying average cell currents.

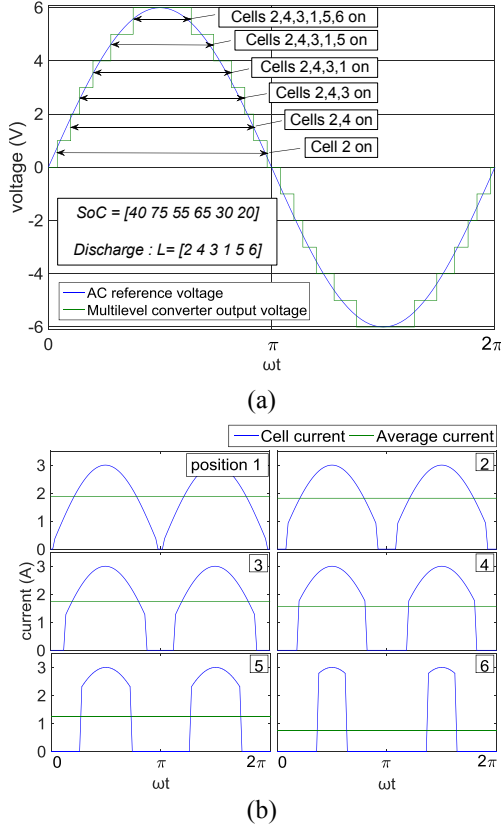


Fig. 2. (a) Output voltage of a 13 level converter (b) Cell currents according to cell position on the priority list. Example numerical value for the SoC given assuming system is discharging.

In [20] a balancing strategy is presented where the above property of the multilevel converter is used in order to enforce different cell currents by controlling the position of each cell

in the *priority list* L , referred to as *cell position*. A voltage matching algorithm is then used in order to achieve a converter output voltage close to the sinusoidal reference by switching on the appropriate number of cells, according to the priority list.

When charging, balancing is achieved by placing cells with lower relative SoC (RSoC) closer to the beginning of the priority list (cell position closer to 1). This leads to the voltage matching algorithm using cells with lower RSoC for a greater length of time during each half cycle of the grid waveform. As a result, charge is inserted into these cells at a higher average rate (higher average cell current) when compared to cells with a higher RSoC, which will be further down the priority list and so used by the voltage matching algorithm for shorter periods of time in each half cycle. This process is illustrated in Fig. 2. When discharging, the priority list is sorted in reverse order so that cells with higher RSoC are discharged with higher average cell currents than those with low RSoC.

III. CELL BALANCING USING POCV MEASUREMENTS

The effectiveness of a cell balancing strategy is highly dependent on accurate cell RSoC estimation [24]. The OCV measurements could provide the information needed to estimate the relative cell SoC but would require each cell to be removed from the current path for a considerable time [9], which is not possible during operation of conventional battery packs (that include cells connected in series). From Fig. 2b it can be seen that although cell currents vary depending on cell position, during the zero crossings all cell currents are zero. An intuitive way to achieve accurate RSoC estimation is by exploiting these periods to eliminate the effect of the internal cell resistance on cell voltage measurements [19]. If a cell is well modelled only by a series resistance, the measured voltage at the zero crossing would be equal to the OCV; however due to cell dynamics (with time constants of the order 100 ms), the measured cell voltage is affected by the recent current flow history of the cell.

The proposed balancing strategy uses the modularity of the cascaded full bridge multilevel converter in order to enable POCV measurements. With appropriate control of each full bridge converter module, any single cell can be bypassed (i.e. removed from the current path) for a predefined period of time, referred to as the *idle state*, without interrupting operation of the BESS. During the idle state, the effect of the internal cell resistance and transient phenomena shorter than the duration of the idle state can be neglected. This RSoC estimation method is also applicable in CHB multilevel converters with packs of cells connected to each H-bridge, provided that these packs are equipped with voltage sensors for each individual cell. This balancing concept is explained using the equivalent cell circuit model presented in Fig. 3a.

The equivalent circuit consists of a controlled voltage source, a series resistance and a number of RC networks depending on the modelling accuracy required [25]. The voltage source V_{OC} represents the OCV of the cell as a function of cell SoC. The series resistance R_0 is used to represent the internal resistance of the cell. The RC branches model the transient behaviour (time constants) associated with

diffusion (long time constant typically tens of seconds to minutes, $\tau_L = R_L C_L$) and charge transfer phenomena (short time constant typically tens of milliseconds to seconds, $\tau_S = R_S C_S$) within the cell [10].

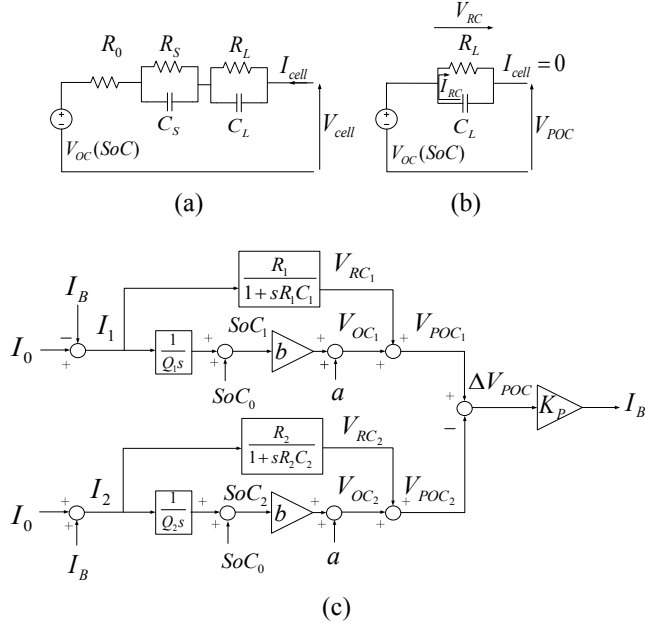


Fig. 3. (a) Generalized equivalent RC circuit (b) Equivalent circuit during idle state (V_{OC} is a function of SoC) (c) POCV balancing scheme implemented on two cells.

With the introduction of the idle state, the effect of the series resistance and the short time constant RC circuits can be neglected so the equivalent circuit is simplified as presented in Fig. 3b. Although the battery current is zero during the idle state, the measured cell voltage is not equal to the true OCV due to the voltage drop caused by the circulating current in the long time constant RC section, thus it is referred to as pseudo-OCV.

In order to estimate the performance of the proposed balancing scheme, a simplified linear model is constructed. This model contains two cells of different capacities and with different time constants as shown in Fig. 3c. Each cell is charged or discharged under a constant current I_0 (depending on the C rate) modified by the balancing current I_B . To preserve linearity, a linear relationship between OCV and SoC is assumed ($V_{OC} = a + bSoC$) and a proportional gain K_P is used to determine the balancing current from the POCV difference.

Under these assumptions, the final value of the POCV difference is described by (1) and the effectiveness of the POCV balancing scheme can be evaluated from the final value of the OCV difference (2).

$$\Delta V_{POC}^* = \lim_{s \rightarrow 0} s \Delta V_{POC}(s) = \frac{I_0(Q_2 - Q_1)}{K_P(Q_1 + Q_2)} \quad (1)$$

$$\begin{aligned} \Delta V_{OC}^* &= \lim_{s \rightarrow 0} s \Delta V_{OC}(s) \\ &= \frac{\frac{I_0}{K_P}(Q_2 - Q_1) + 2I_0(Q_2 R_2 - Q_1 R_1)}{(Q_1 + Q_2)} \end{aligned} \quad (2)$$

Where Q_1, Q_2 are the nominal cell capacities and R_1, R_2 are the respective transient resistances.

Based on (2), the effectiveness of the proposed POCV balancing scheme depends on the applied C rate (I_0), the variation between cell parameters (cell capacity and the transient resistance) and the balancing gain K_P . In the actual system, the cells are operated under different average currents based on the respective cell position. Each cell position corresponds to a specific average current and therefore for very low POCV difference between the cells, K_P is effectively very large. This is because a difference of a single mV in ΔV_{POC} causes the cells to occupy different places in the priority list and therefore to experience non zero balancing currents. As a result, ΔV_{POC} and ΔV_{OC} are described by (3) and (4) for the real system.

$$\lim_{K_P \rightarrow \infty} \Delta V_{POC}^* = 0 \quad (3)$$

$$\lim_{K_P \rightarrow \infty} \Delta V_{OC}^* = \frac{2I_0(Q_2 R_2 - Q_1 R_1)}{Q_1 + Q_2} \quad (4)$$

According to (4), ΔV_{OC} is zero for identical cells (i.e. cells with equal transient resistance and capacity), so POCV balancing is expected to lead to OCV and thus SoC balancing.

However, due to aging, cell capacity and the equivalent circuit parameters can vary. These variations in cell capacity and circuit parameters introduce a voltage difference between OCVs (4). A study regarding the effect of cell aging in the parameters of a lithium ion cell is presented in [26]. A monotonic increase is observed in the total resistance and the diffusion time constant whereas the capacity of the cell is monotonically decreasing. The change in cell parameters over 3000 and 6000 cycles is presented in Table 1.

TABLE I CELL PARAMETER VARIATION DUE TO AGING (FROM [26])			
Number of cycles	0	3000	6000
Cell capacity	Q_n	$0.85Q_n$	$0.75Q_n$
Cell resistance	R_n	$1.5R_n$	$2R_n$
Diffusion time constant	τ_n	$1.25\tau_n$	$1.6\tau_n$

Where Q_n is the nominal cell capacity at 0 cycles, R_n is the nominal cell resistance and τ_n is the nominal value of the diffusion time constant.

Equation (4) can be used to estimate the SoC difference (i.e. balancing error) arising from the system attempting to balance mismatched cells. The OCV difference after POCV balancing of a new and an aged cell (after 6000 cycles) assuming operation at a 1C rate, a nominal capacity of $Q_n = 2.2$ Ah and a nominal cell transient resistance $R_n = 10$ m Ω is 12.6 mV. The corresponding SoC difference depends on the slope of the OCV-SoC curve for the particular cell chemistry under examination. The SoC difference for the lithium polymer cells used in this study is maximum near 50% SoC (where 12.6mV corresponds to a 6.64% balancing error), and minimum at the 10% and 90% ranges (where 12.6mV corresponds to a 1.25% balancing error).

A. Selecting the duration of the idle state

The idle state duration should be set short enough so that high quality POCV measurements can be taken without increasing the SoC difference between cells (due to different average cell currents) but long enough to ensure that the voltage drop across the short time constant RC network can be neglected. In order to choose a suitable idle state duration, the switching strategy of the multilevel converter is considered. In the cascaded multilevel converter, the peak value of the output voltage waveform depends on the maximum number of available converter cells (5):

$$V_{peak} = N_{on} V_{cell} \quad (5)$$

Where V_{peak} is the peak value of the reference voltage waveform, N_{on} is the maximum number of available cells and V_{cell} is the nominal voltage of the cells.

A new cell is switched on in order to achieve an output converter voltage closer to the sinusoidal voltage reference than before (with that cell off), the switching angle α_i can be found by substituting (5) in (6) and solving for α_i .

$$V_{peak} \cos(\alpha_i) = V_{cell}(i - 0.5), \quad i = 1..N_{on} \quad (6)$$

$$\alpha_i = \arccos\left(\frac{i - 0.5}{N_{on}}\right) \quad (7)$$

Considering the symmetry of a sinusoidal waveform, the average cell current over half a fundamental period is calculated by (8) for the different cell positions.

$$I_{cell}(i) = \frac{1}{\pi} \int_{-T/4}^{T/4} \sqrt{2} I_{rms} \cos(\theta - \varphi) d\theta \quad (8)$$

$$= \frac{2\sqrt{2}}{\pi} I_{rms} \cos(\varphi) \sqrt{1 - \left(\frac{i - 0.5}{N_{on}}\right)^2}$$

Where I_{rms} is the RMS current of the multilevel converter and $\cos(\varphi)$ is the power factor of the load.

In this paper, a twelve cell multilevel converter is considered with $N_{on} = 10$, $\sqrt{2}I_{rms} = 3$ A, $\cos(\varphi) = 1$. Although the system includes 12 cells, the number of the available cell positions is 10 as one cell is always at the idle state and to allow the system to tolerate failure of one cell. The maximum and minimum average cell currents can be calculated as follows (9)-(10).

$$I_{max} = I_{cell}(1) = 1.91 \text{ A} \quad (9)$$

$$I_{min} = 0 \text{ A (redundant cell)} \quad (10)$$

The upper limit for the duration of the idle state is selected so that SoC variation due to unequal (dis)charge rates across cells does not exceed 1%, between two consecutive POCV measurement updates. The maximum SoC variation is observed between a cell operating under the maximum cell current and a cell remaining idle and can be found by solving (11).

$$I_{max} t_i (N_{on} - 1) \leq 0.01 Q_n 3600 \quad (11)$$

Where t_i is the idle state duration in sec ($t_i(N_{on} - 1)$ is the duration between two consecutive POCV measurements) and Q_n is the nominal capacity of the cell in Ampere-hours (Ah) equal to 2.2 Ah.

By solving (11) for t_i , the maximum idle state duration is 4.6 sec. According to [27] the charge transfer time constant of lithium polymer cells is 0.12 - 0.46 s depending on cell SoC. As a result, the duration of the idle state is selected to be 3 seconds to ensure that the effect of the short time constant may be neglected whilst also limiting the SoC difference between cells.

IV. SIMULATION RESULTS OF THE PROPOSED BALANCING STRATEGY

In order to validate the concept of POCV and quantify the effect of large time constants on cell balancing, the equivalent RC circuit of a 2.2 Ah Lithium polymer cell is developed and used for simulation. The equivalent circuit model is used to simulate the cases of balancing between twelve identical new cells with a 55% initial SoC variation and balancing between eleven new and one aged cell (using the data from Table 2) with the same initial SoC variation. A first order equivalent RC circuit is typically considered a good compromise between accuracy and computational demands [28]. To simplify the study, an equivalent circuit with constant parameters over the range of SoC is used. Based on [29] the constant parameters can be calculated by minimizing the squared error between the measured cell voltage and the cell voltage calculated using the equivalent circuit model. The resulting parameters for the equivalent RC circuit are given in Table 2.

TABLE II
CALCULATED PARAMETERS OF THE EQUIVALENT RC CIRCUIT MODEL

Parameter	Symbol	Value
Series resistance	R_0	18.4 mΩ
Transient resistance	R_{RC}	7.72 mΩ
Diffusion time constant	τ_{RC}	45.0 s

In both simulations the initial cell SoC are evenly spread between 85 and 30%. In the case of balancing between twelve identical cells (Fig. 4a), POCV balancing is achieved at 64 min. During the first discharge cycle, the cells with the highest POCVs are discharged with higher currents but when the charging cycle begins, priority is given to the cells with lower POCVs. In this case, the close agreement between the transient resistances of the cells combined with the equal cell capacities results in accurate OCV balancing ($\Delta V_{OC} = 0$).

In the second simulation, the parameters of cell 12 are set based on Table 2, in order to simulate an aged cell (i.e. a cell that has experienced 6000 cycles). POCV balancing is achieved at 68 min and is retained throughout the simulation. In this case however, the POCV balancing does not lead to a perfect OCV balancing because of the different V_{RC} between the aged cell and all other cells. In order to balance the POCVs, a lower cell current is applied to the aged cell (cell 12 with decreased capacity). This current combined with the increased cell resistance (the internal resistance is doubled

based on Table 1) introduces a voltage difference ΔV_{RC} of 4 to 6 mV that corresponds to the OCV difference. This difference in OCV is translated to a 0.8 % difference in SoC between the cells at the end of each cycle using Fig. 4b. A close agreement is observed in this case, as the effect of the decreased average current of the aged cell is negated to some extent by the simultaneous increase in the transient resistance. Using (4) the OCV difference between the cells is calculated at 4.95 mV, thus a good agreement is observed between simulation and the theoretical calculations. Simulations also confirm the dependence of cell balancing on the C rate. The OCV error tends to increase proportionally with the C rate as indicated by (4). However the SoC error at the end of a (dis)charge cycle is less than 3.5% for up to 2 C rate.

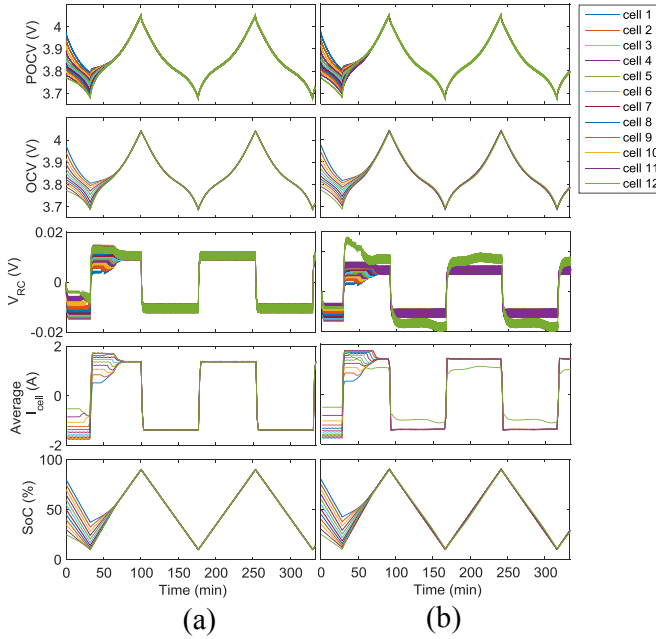


Fig. 4. POCV, OCV, V_{RC} , average I_{cell} and SoC for the balancing of (a) Twelve identical new cells and (b) Eleven identical new cells and an aged cell (after 6000 cycles based on Table 1).

V. CONVERTER CONTROL USING THE CELL BALANCING ALGORITHM

The adopted balancing strategy is described in Fig. 5a. The balancing strategy consists of two parallel operations at different execution rates: A slow process of disabling a cell every 3 seconds (idle state) followed by the cell sorting and fast processes (50 kHz) including cell voltage measurements, nearest voltage matching and switching signal generation.

At the end of idle state, the measured cell voltage is used to update the POCV measurements of the disabled cell. The POCV of each cell is used during the process of cell sorting, when the cells are sorted in ascending or descending order of POCV, depending on the operation (discharging or charging). The output voltage is then synthesized based on the nearest voltage matching algorithm. The algorithm minimizes the error between the reference voltage and the converter's output voltage by switching on the appropriate number of cells following the priority list (Fig. 5a).

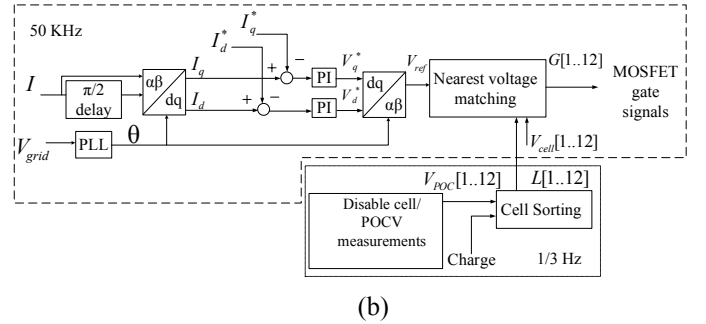
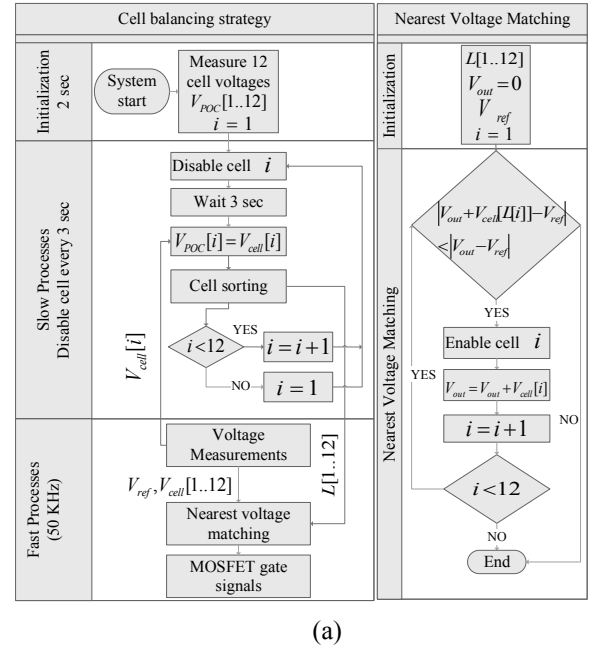


Fig. 5. (a) Description of the proposed cell balancing strategy (b) Complete control of the single phase multilevel converter prototype.

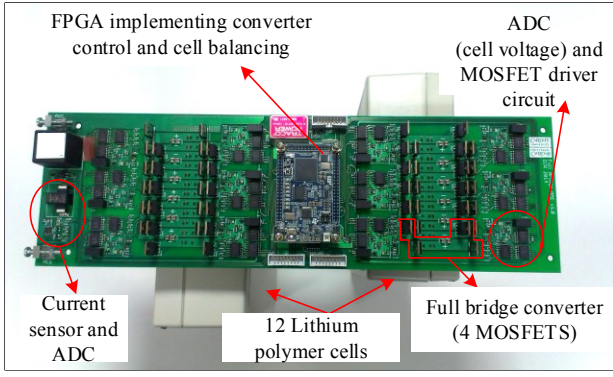
The complete control of the single phase full bridge multilevel converter is presented in Fig. 5b. A single-phase phase locked loop (PLL) described in [30] is used to synchronize with the angle of the grid voltage θ . Cell current is controlled using two PI controllers to control the d-axis and q-axis components of the current. The q-axis current reference is set to zero to achieve output with unity power factor. The d-axis current reference is set to the desired charging/discharging current magnitude. The output of the PI controllers corresponds to the respective d-q axis components of the reference voltage. After the reverse Park transformation, the reference output voltage is acquired. This voltage is used as input for the nearest voltage matching algorithm where the switching sequence of the cells is decided according to the balancing methodology presented in Fig. 5a.

VI. EXPERIMENTAL VALIDATION

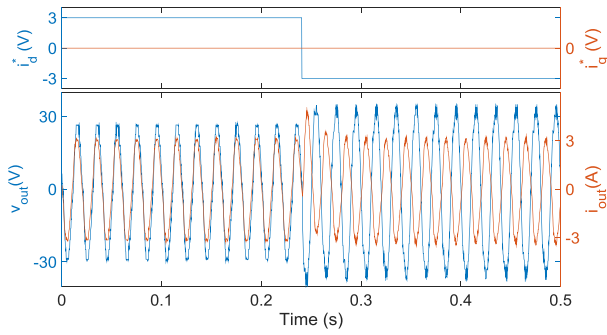
In order to verify the performance of the proposed balancing strategy based on POCV measurements, a single phase 12 cell cascaded full bridge multilevel converter is used. Each full bridge converter module is connected to a single 2.2 Ah lithium polymer cell. The converter control and the individual cell balancing algorithm are implemented in an

FPGA device located on the PCB (Fig. 6a). The experimental procedure is described as follows:

- 1) Prior to each test, all twelve cells are discharged from 100% SoC to different SoC values between 75-20%. After discharge the cells are left to rest for 30 min in order to measure their OCV.
- 2) Consecutive charging and discharging cycles: The single phase multilevel converter is connected to the grid. The current reference is set as $I_d^* = 3$ A, $I_q^* = 0$ A for charging and $I_d^* = -3$ A, $I_q^* = 0$ A for discharging. The controller is set to operate the cells in consecutive charging and discharging cycles between the following POCV limits: $POCV_{max} = 3.9$ V, $POCV_{min} = 3.7$ V. This corresponds to consecutive cycles between 15% and 65% SoC. The above POCV limits are selected in order to ensure that the terminal voltage of any cell does not exceed the suggested voltage limits (3V and 4.2 V) at any point during operation. After five consecutive cycles, operation is terminated and the cells are left to rest for 20 min. The results from two tests are presented here: balancing of twelve 2.2 Ah cells and balancing of eleven 2.2 Ah cells and a 1 Ah cell.



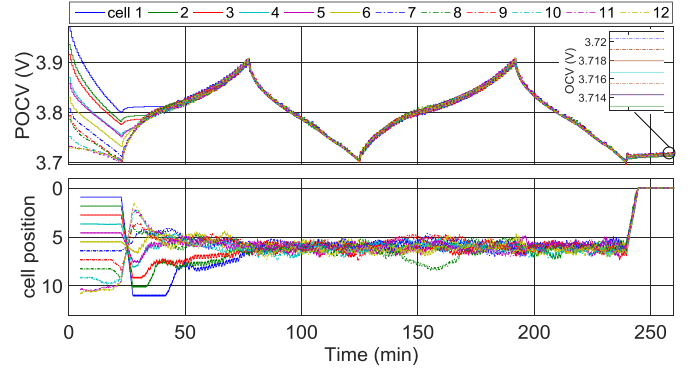
(a)



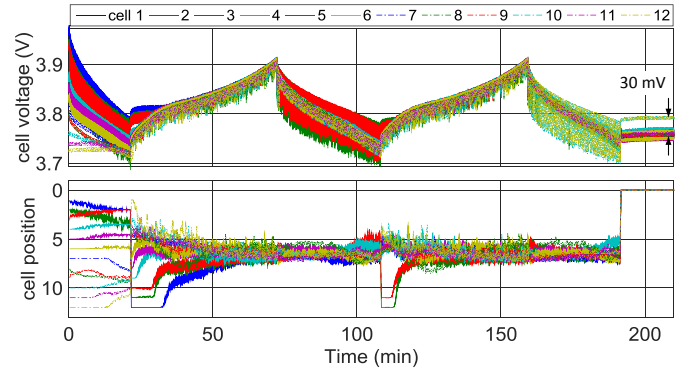
(b)

Fig. 6. (a) 25 level cascaded full bridge multilevel converter prototype (b) Experimental multilevel converter output voltage and current during the transition between charging and discharging.

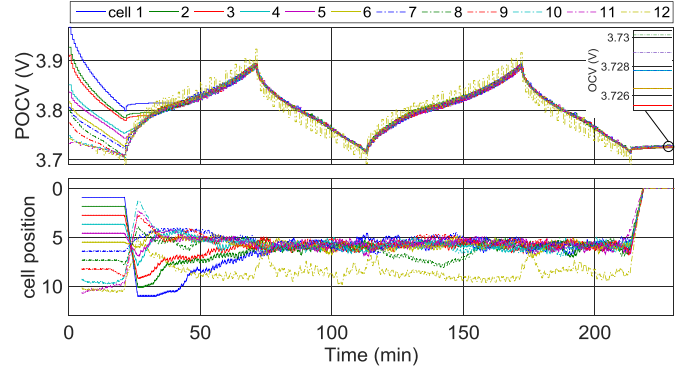
VII. RESULTS AND DISCUSSION



(a)



(b)



(c)

Fig. 7. POCV (cell voltage) and average cell position over 100 samples for the balancing test of (a) Twelve cells with a 2.2 Ah nominal capacity (b) Twelve cells with a 2.2 Ah nominal capacity, without using the idle state for POCV measurements. (c) Eleven cells with a 2.2 Ah nominal capacity and a cell with a 1 Ah nominal capacity

A. Balancing of twelve 2.2 Ah cells

The different POCVs of the twelve cells (Fig. 7a) at the beginning of the test correspond to the initial SoC variation between the cells. During discharge, cells with the highest POCVs (cells 1-3) are considered high priority cells and are placed in the highest cell positions (closer to one) in order to be discharged with higher cell currents. Discharge operation is terminated when $POCV_{min}$ is reached by cell 11 and the first charging cycle begins. The multilevel converter output voltage

and current at the transition between discharging and charging is presented in Fig. 6b. As the output is constant current, the increase in converter output voltage observed during discharge (due to grid impedance) leads to a higher discharge rate at 0.6 C (0.45 C during charging). During charging, priority is given to the cells with the lowest POCVs (cells 10-12) which are now placed in the higher cell positions. POCV balancing is achieved around 40 min.

In order for the cells to remain balanced, the algorithm needs to respond rapidly to POCV deviations by adjusting cell position. Balancing is retained by operating the cells equally as indicated by the close agreement in average cell position. The adaptiveness of the balancing is demonstrated around 150 min where the position of cell 8 is adjusted to lower values in order to compensate for the decreased capacity of the cell compared to the rest (2 Ah measured cell capacity for cell 8 compared to 2.2 Ah nominal capacity). After the end of the third discharge cycle the cells are left to rest for 20 min. The effectiveness of the balancing strategy is verified by the close agreement of the measured OCV (within 8 mV).

In order to demonstrate the effect of the short time constant on cell balancing, the previous test is repeated but instead of the POCV, balancing is now performed using the cell voltage measured during the zero crossings (Fig. 2). The negative effect of the low quality voltage measurements used here is evident during the discharge cycles. During the first discharge cycle (72-108 min) the voltages of cells 2 and 3 alternate, causing the cells to be placed constantly either on the first or the last cell position. As a result the cells are always discharged either with the highest or with the lowest cell current, maintaining a voltage fluctuation that can reach up to 80 mV. Due to the low quality of voltage measurements, the SoC variation between these two cells and the rest cannot be detected by the balancing algorithm and therefore the cells are equally discharged as indicated by the close agreement of the average cell position (Fig. 7b). Similar behaviour is observed during the second discharge cycle (159-191 min) between cells 10 and 12. After the end of the test a 30 mV difference is observed between the voltages of these two cells and the rest, as indicated by Fig. 7b.

B. Balancing of eleven 2.2 Ah cells and a 1 Ah cell

In this experiment cell 12 is replaced with a 1 Ah cell (45% of the capacity of the other cells). The operation of the multilevel converter is presented in Fig. 7c. The balancing strategy in this case is expected to overcome the initial SoC imbalance between the cells and the difference in cell capacity. During discharge the balancing algorithm ensures that cells with the higher POCVs (cells 1-3) are placed on higher cell position (higher discharge current). When charging the cell position is reversed and cells with the lower POCVs (cells 9-11) are placed on top of the priority list. POCV balancing in this test is achieved at 40 min. In this test a high fluctuation in POCV measurements is observed for cell 12 (the low capacity cell). The reason for this is the difference in cell capacity that causes it to experience rapid changes in SoC between two consecutive POCV measurements (36 seconds), compared to the other cells. These rapid SoC changes are reflected in the OCV and can be observed in the measured POCV. Based on the estimated SoC and the observed cell

position, cell balancing is achieved around 75 min. In order for the cells to remain balanced, the average cell position of cells 1-11 is close to 6 whereas the average cell position of cell 12 is significantly lower (between 8 and 10) due to the decreased cell capacity. An adjustment in the cell position of cell 8 is also observed in this test around 130 min. Once the discharge process ends at 210 min, the cells are disconnected from the grid and left to rest. The good agreement between OCVs (within 5 mV) demonstrates that the balancing strategy can tolerate very large capacity variation.

VIII. CONCLUSION

This paper has presented a methodology of cell balancing using a cascaded full bridge multilevel converter where a single cell is connected to each converter module allowing individual cell monitoring and control. In this approach cell balancing is achieved by controlling the position of each cell in a priority list and therefore the average cell current, based on the relative SoC. In order to accurately estimate the relative cell SoC, the concept of an idle state was introduced. During the idle state, the cell is temporarily removed from the current path for a short period of time. As a result, the effect of the series resistance and short time transient phenomena can be neglected and therefore cell voltage measurements taken during the idle state can be used as a pseudo-OCV measurement. The effectiveness of the proposed POCV balancing depends on the applied C rate and the difference in cell capacities and transient resistance. Simulation results demonstrate a successful balancing to within 0.8 % of SoC between cells operated at 0.5 C and 3.5 % for cells at 2 C, with 55% initial SoC variation and up to 25% difference in nominal capacity. The proposed strategy was validated experimentally using a 25 level cascaded full bridge multilevel converter prototype for the balancing of 12 lithium polymer cells during consecutive charging and discharging cycles. A balancing within 5 mV of the OCV was observed between cells with 55% initial SoC variation and 45% capacity difference.

REFERENCES

- [1] F. Díaz-González, A. Sumper, O. Gomis-Bellmunt, and R. Villafañila-Robles, "A review of energy storage technologies for wind power applications," *Renewable and Sustainable Energy Reviews*, vol. 16, pp. 2154-2171, 2012.
- [2] V. Férnão Pires, E. Romero-Cadaval, D. Vinnikov, I. Roasto, and J. F. Martins, "Power converter interfaces for electrochemical energy storage systems – A review," *Energy Conversion and Management*, vol. 86, pp. 453-475, 10// 2014.
- [3] G. J. Offer, V. Yufit, D. A. Howey, B. Wu, and N. P. Brandon, "Module design and fault diagnosis in electric vehicle batteries," *Journal of Power Sources*, vol. 206, pp. 383-392, 2012.
- [4] B. Kenney, K. Darcovich, D. D. MacNeil, and I. J. Davidson, "Modelling the impact of variations in electrode manufacturing on lithium-ion battery modules," *Journal of Power Sources*, vol. 213, pp. 391-401, 2012.
- [5] L. Lu, X. Han, J. Li, J. Hua, and M. Ouyang, "A review on the key issues for lithium-ion battery management in electric vehicles," *Journal of power sources*, vol. 226, pp. 272-288, 2013.
- [6] J. Cao, N. Schofield, and A. Emadi, "Battery balancing methods: A comprehensive review," in *Vehicle Power and Propulsion Conference, 2008. VPPC '08. IEEE*, 2008, pp. 1-6.
- [7] K. Kutluay, Y. Cadirci, Y. S. Özkazanç, and I. Cadirci, "A new online state-of-charge estimation and monitoring system for sealed lead-acid batteries in telecommunication power supplies," *Industrial Electronics, IEEE Transactions on*, vol. 52, pp. 1315-1327, 2005.

- [8] M. Charkhgard and M. Farrokhi, "State-of-charge estimation for lithium-ion batteries using neural networks and EKF," *Industrial Electronics, IEEE Transactions on*, vol. 57, pp. 4178-4187, 2010.
- [9] Y. Xing, W. He, M. Pecht, and K. L. Tsui, "State of charge estimation of lithium-ion batteries using the open-circuit voltage at various ambient temperatures," *Applied Energy*, vol. 113, pp. 106-115, 2014.
- [10] C. Fleischer, W. Waag, H.-M. Heyn, and D. U. Sauer, "On-line adaptive battery impedance parameter and state estimation considering physical principles in reduced order equivalent circuit battery models: Part 1. Requirements, critical review of methods and modeling," *Journal of Power Sources*, vol. 260, pp. 276-291, 2014.
- [11] G. L. Plett, "Extended Kalman filtering for battery management systems of LiPB-based HEV battery packs: Part 2. Modeling and identification," *Journal of power sources*, vol. 134, pp. 262-276, 2004.
- [12] I.-S. Kim, "The novel state of charge estimation method for lithium battery using sliding mode observer," *Journal of Power Sources*, vol. 163, pp. 584-590, 2006.
- [13] N. Kawakami, S. Ota, H. Kon, S. Konno, H. Akagi, H. Kobayashi, *et al.*, "Development of a 500-kW Modular Multilevel Cascade Converter for Battery Energy Storage Systems," *Industry Applications, IEEE Transactions on*, vol. 50, pp. 3902-3910, 2014.
- [14] M. Vasiladiotis and A. Rufer, "Balancing control actions for cascaded H-bridge converters with integrated battery energy storage," in *Power Electronics and Applications (EPE), 2013 15th European Conference on*, 2013, pp. 1-10.
- [15] M. Vasiladiotis and A. Rufer, "Analysis and control of modular multilevel converters with integrated battery energy storage," *Power Electronics, IEEE Transactions on*, vol. 30, pp. 163-175, 2015.
- [16] L. Maharjan, S. Inoue, H. Akagi, and J. Asakura, "State-of-charge (SOC)-balancing control of a battery energy storage system based on a cascade PWM converter," *Power Electronics, IEEE Transactions on*, vol. 24, pp. 1628-1636, 2009.
- [17] C.-M. Young, N.-Y. Chu, L.-R. Chen, Y.-C. Hsiao, and C.-Z. Li, "A single-phase multilevel inverter with battery balancing," *Industrial Electronics, IEEE Transactions on*, vol. 60, pp. 1972-1978, 2013.
- [18] L. Maharjan, T. Yamagishi, and H. Akagi, "Active-power control of individual converter cells for a battery energy storage system based on a multilevel cascade PWM converter," *Power Electronics, IEEE Transactions on*, vol. 27, pp. 1099-1107, 2012.
- [19] M. Chen, B. Zhang, Y. Li, G. Qi, and J. Liu, "Design of a multi-level battery management system for a Cascade H-bridge energy storage system," in *Power and Energy Engineering Conference (APPEEC), 2014 IEEE PES Asia-Pacific*, 2014, pp. 1-5.
- [20] C. A. Ooi, D. Rogers, and N. Jenkins, "Balancing control for grid-scale battery energy storage system," *Proceedings of the Institution of Civil Engineers-Energy*, vol. 168, pp. 145-157, 2015.
- [21] V. V. Viswanathan and M. Kintner-Meyer, "Second use of transportation batteries: Maximizing the value of batteries for transportation and grid services," *Vehicular Technology, IEEE Transactions on*, vol. 60, pp. 2963-2970, 2011.
- [22] C. R. Birkel, D. F. Frost, A. M. Bizeray, R. R. Richardson, and D. A. Howey, "Modular converter system for low-cost off-grid energy storage using second life li-ion batteries," in *Global Humanitarian Technology Conference (GHTC), 2014 IEEE*, 2014, pp. 192-199.
- [23] T. Kim, W. Qiao, and L. Qu, "A multicell battery system design for electric and plug-in hybrid electric vehicles," in *Electric Vehicle Conference (IEVC), 2012 IEEE International*, 2012, pp. 1-7.
- [24] S. Tong, M. P. Klein, and J. W. Park, "On-line optimization of battery open circuit voltage for improved state-of-charge and state-of-health estimation," *Journal of Power Sources*, vol. 293, pp. 416-428, 2015.
- [25] M. Chen and G. A. Rincon-Mora, "Accurate electrical battery model capable of predicting runtime and IV performance," *Energy conversion, IEEE transactions on*, vol. 21, pp. 504-511, 2006.
- [26] G. K. Prasad and C. D. Rahn, "Model based identification of aging parameters in lithium ion batteries," *Journal of power sources*, vol. 232, pp. 79-85, 2013.
- [27] J.-H. Lee and W. Choi, "Novel state-of-charge estimation method for lithium polymer batteries using electrochemical impedance spectroscopy," *Journal of Power Electronics*, vol. 11, pp. 237-243, 2011.
- [28] X. Hu, S. Li, and H. Peng, "A comparative study of equivalent circuit models for Li-ion batteries," *Journal of Power Sources*, vol. 198, pp. 359-367, 2012.
- [29] J. Li and M. S. Mazzola, "Accurate battery pack modeling for automotive applications," *Journal of Power Sources*, vol. 237, pp. 215-228, 2013.
- [30] M. Ciobotaru, R. Teodorescu, and F. Blaabjerg, "Improved PLL structures for single-phase grid inverters," *Proc. of PELINCEC*, vol. 5, 2005.



Efstratios Chatzinikolaou (S'16) received the Diploma degree in electrical and computer engineering from National Technical University of Athens, Athens, Greece, in 2013. Currently, he is reading for DPhil in Engineering Science at the University of Oxford, U.K. His research interests include modular multilevel converter topologies and power electronic interfaces for battery energy storage systems.



Daniel J. Rogers (M'09) received the M.Eng. and Ph.D. degrees in electrical and electronic engineering from Imperial College London, London, U.K., in 2007 and 2011 respectively. Currently, he is a Senior Research Fellow at the University of Oxford, U.K. He conducts research in collaboration with industry and is an investigator on EPSRC and EU research projects in the areas of power electronics, HVDC and grid-scale energy storage. His research interests include the use of medium- and large-scale power electronic systems to create flexible electrical networks capable of taking advantage of a diverse range of generation technologies.